



Train post-derailment behaviours and containment methods: a review

Zhao Tang¹ · Yuwei Hu¹ · Shuangbu Wang² · Liang Ling¹ · Jianjun Zhang³ · Kaiyun Wang¹

Received: 23 March 2023 / Revised: 5 June 2023 / Accepted: 6 June 2023
© The Author(s) 2023

Abstract

Railway accidents, particularly serious derailments, can lead to catastrophic consequences. Therefore, it is essential to prevent derailment escalation to reduce the likelihood of severe derailments. Train post-derailment behaviours and containment methods play a critical role in preventing derailment escalation and providing passive safety protection and accident prevention in the event of a derailment. However, despite the increasing attention on this field from academia and industry in recent years, there is a lack of systematic exploration and summarization of emerging applications and containment methods in train post-derailment research. For this reason, this paper presents a comprehensive review of existing studies on train post-derailment behaviours, encompassing various topics such as post-derailment contact–impact models, dynamic modelling and simulation techniques, and the primary factors influencing post-derailment behaviours. Significantly, this review introduces and elucidates substitute guidance mechanisms (SGMs), which serve as railway-specific passive safety protection and accident prevention measures. The various types of SGMs are depicted, and their ongoing developments and applications are explored in depth. The review additionally points out several unresolved challenges including the adverse effects of SGMs, and proposes future research directions to advance the theoretical understanding and practical application of train post-derailment behaviours and containment methods. This review seeks to be a valuable reference for railway industry professionals in preventing catastrophic derailment consequences through post-derailment containment methods.

Keywords Railway passive safety · Railway accident prevention · Post-derailment behaviours · Substitute guidance mechanisms (SGMs) · Contact–impact model

1 Introduction

1.1 Background

Derailments are the most common type of train accident [1–3]. According to statistics from the Federal Railroad Administration (FRA) [4], derailment accidents accounted for over 60% of all serious railway accidents in the USA. In other regions, such as Europe and China, the International Union of Railways (UIC) and European Union Agency for

Railways (ERA) report derailment accidents also account for a significant proportion of total railway accidents [5, 6].

Derailment accidents can be classified into two categories: on-track and off-track. On-track derailments occur when derailed cars slide off the rails but remain on the railway track. Although this type of derailment accident is the most common, it typically results in minimal injuries or railway transportation delays and presents a relatively low risk to passenger safety.

In contrast, off-track derailments occur when a part or the whole train not only runs off the rail but also completely veers off the railway tracks. This type of derailment is far more severe and can lead to the train tipping over or rolling over, colliding with catenary pillars, buildings, stations, or other objects within or near the railway line, and even falling under a viaduct. Off-track derailment accidents can cause catastrophic consequences and result in heavy loss of human life and property. Figure 1 depicts several notable off-track derailment accidents that took place between 2017 and 2023, leading to 21 fatalities and hundreds of injuries.

✉ Zhao Tang
tangzhao@swjtu.edu.cn

¹ State Key Laboratory of Traction Power, Southwest Jiaotong University, Chengdu 610031, China

² Institute of Smart City and Intelligent Transportation, Southwest Jiaotong University, Chengdu 610031, China

³ National Centre for Computer Animation, Bournemouth University, Dorset, UK

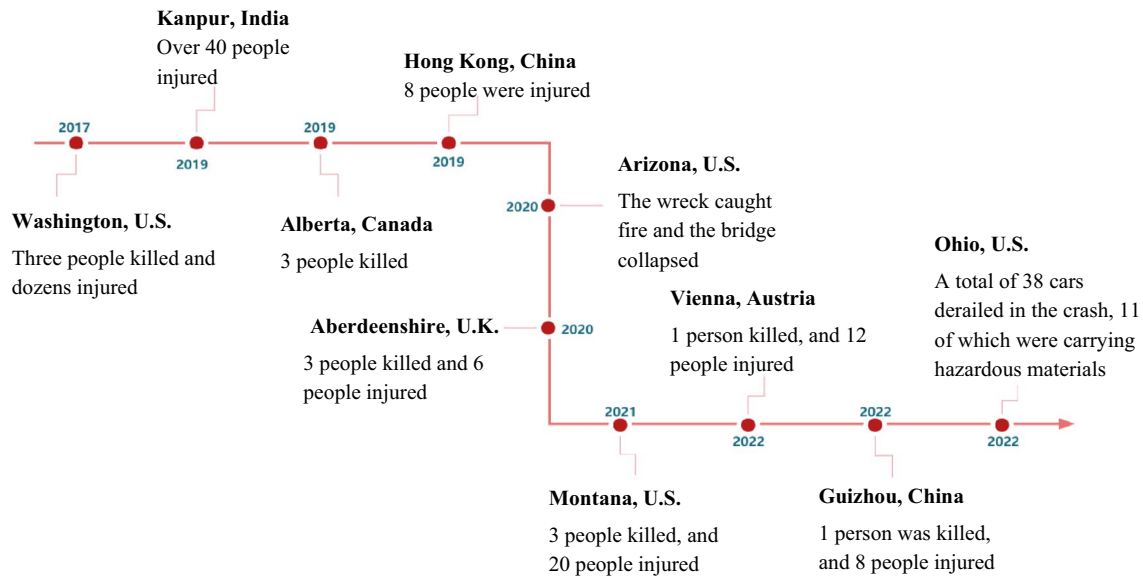


Fig. 1 Off-track derailment accidents in recent years

In particular, the recent Ohio derailment caused significant environmental concerns due to a large chemical spill that posed a serious threat to the ecosystem.

Upon thoroughly analysing the off-track derailments depicted in Fig. 1, it becomes evident that the post-derailment behaviours resulting in fatal consequences are diverse and complex. These behaviours include falling off a bridge, colliding with lineside infrastructure, striking a landslip, and crashing into a railway bridge deck. Gaining a comprehensive understanding of these post-derailment behaviours is essential for enhancing railway safety and minimizing the impact of off-track derailment accidents.

In theory, preventing derailment is an ideal solution to avoid such accidents. However, the loosely coupled wheel–rail relationship makes it almost impossible to completely avoid the occurrence of derailment accidents. Therefore, it is important to focus on reducing the occurrence of off-track derailments and minimizing their consequences through passive safety protection and accident prevention measures. The derailment of a Shinkansen train caused by an earthquake on 23 October 2004 [7] brought attention to the significance of post-derailment studies among railway safety researchers. As shown in Fig. 2, the wheels of the train pinned the rails against the lifeguard of the lead car, bringing the train to a halt without veering off the track and ultimately preventing an off-track derailment accident.

1.2 Concept and scope of the post-derailment study

The study of train post-derailment behaviours is an essential aspect of railway passive safety, as it aims to provide effective containment methods to minimize the consequences



Fig. 2 The derailment accident of a Shinkansen train, in operation since 1964, which highlighted the need for increased focus on train post-derailment studies in both academic and industrial sectors [7]

of derailment accidents. Post-derailment studies primarily focus on understanding the dynamic behaviours of a train after a derailment occurs. The objective of post-derailment investigations is to develop appropriate countermeasures or containment methods that maintain a train upright position and proximity to the track centreline after a derailment, thereby reducing the incident's severity, preventing further escalation, and mitigating the potential for catastrophic derailment accidents.

Post-derailment studies mainly focus on several key research areas, including dynamic modelling and simulations to represent and analyse train behaviours after derailment events, and the development of contact–impact models that depict interactions between derailed trains and their surroundings. These studies also investigate the design and implementation of substitute guidance mechanisms (SGMs), which are passive safety protection measures for railways, and explore

various testing methods and experimental research in both laboratory and field settings to validate theoretical research findings and refine containment methods accordingly.

2 Post-derailment behaviours of railway rolling stock

2.1 The main influential factors

Figure 3 illustrates the multitude of factors that can influence the behaviour of rolling stock after a derailment. These factors include various vehicle-related parameters, such as train length, weight, and component geometry, as well as railway-related factors such as track geometry and friction coefficient. Other factors, such as marshalling, derailment velocity, and cause, also play a significant role.

There is a correlation between the cause of a derailment and its escalation, specifically in terms of the severity of the derailment accident [8, 9]. By analysing statistics on derailment accidents, it can be observed that the post-derailment behaviour of each derailment is different. Some derailments escalate immediately, while others rarely do. Some derailments escalate at the beginning of the derailment, while others can travel several kilometres before escalating. The cause of the derailment can be one of the reasons for explaining this phenomenon. A report [10] found that some types of derailments, such as track buckle, defective switches, collision, and overspeed, may escalate quickly, while other types of derailments, including broken wheels, wheel climb, bogie defects, etc., escalate slowly. It is evident that the cause of a derailment can be a significant factor that influences the behaviour of rolling stock after the incident.

The speed at which the derailment occurred (herein-after referred to as ‘derailment speed’) also has a significant impact on the post-derailment distance and posture. Derailment kinetic energy is proportional to the square of the derailment speed, so even a small increase in derailment speed can have a huge impact on the post-derailment lateral and longitudinal motion of the vehicle. Reducing the derailment speed has a very positive effect on decreasing the post-derailment distance and severity of the derailment accident, as verified by both numerical simulation [10, 11] and test [12, 13]. However, different derailment speeds can cause the railway component to play different

roles in post-derailment behaviour, as revealed by a full-scale derailment test [13]. In this test, different derailment velocities were selected and compared, and it was found that the humps in the concrete track had an influence on post-derailment behaviour when the test bogie derailed at a lower speed (28.08 km/h), but not at a higher derailment speed (55.05 km/h).

Low-speed post-derailment tests on different types of tracks also revealed that track type has an influence on the post-derailment behaviour of a derailed vehicle. Compared to CRT-I slab ballastless track, CRTS-II ballastless track has a better performance in restricting the lateral motion of a derailed vehicle [12].

According to the studies [14, 15], there is a correlation between train lengths and the severity of derailments. Likewise, full-scale derailment tests have demonstrated that the weight of the leading car has a more significant impact on post-derailment distance compared to the rest of the train [12]. The weight of the train and the coefficient of friction are among the factors that influence the effect of ground resistance on the train, in accordance with Coulomb’s friction law. Furthermore, the post-derailment behaviour is influenced by track geometry, such as sleeper intensity, as reported in Refs. [8, 15].

In summary, the factors influencing post-derailment behaviour are multifaceted and intricate. The precise mechanisms through which these factors affect the post-derailment process are not yet fully understood, and there remain several unknown variables. Additionally, a detailed analysis of the relationship between these factors and post-derailment behaviour is lacking.

2.2 Post-derailment contact–impact behaviours

Describing all contact–impact behaviours that occur after the derailment is the foundation and prerequisite for modelling and simulating post-derailment contact–impact interactions. Post-derailment contact–collision behaviours can be roughly and typically divided into three categories: contact–impact behaviour between the car bodies, contact–impact behaviour between the vehicle components and the railway track, and contact–impact behaviour between the vehicle and surrounding structures.

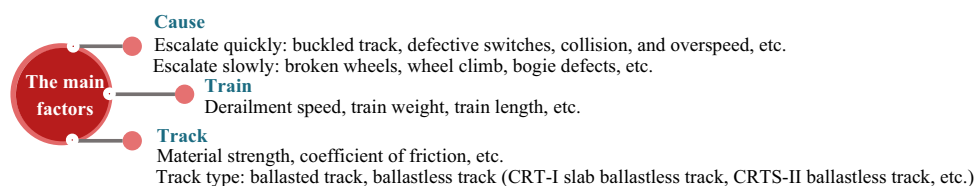


Fig. 3 Main factors that influence the train post-derailment behaviours

2.2.1 Post-derailment contact–impact between the car bodies

When a train derails at high speed, the front derailed vehicle decelerates and rotates, driving the rear vehicle to generate yaw motion one after another. Due to the huge kinetic energy and inertia, large relative rotation and displacement of the vehicle body occur after coupler failure, resulting in contact between the car bodies. Consequently, damage to the car bodies will be produced in the form of penetration, extrusion, and tearing [16–20]. Corner-to-corner contact and corner-to-car body contact are the two main contact pairs between the car bodies, which can be found in authentic accident scene photos (Fig. 4).

2.2.2 Post-derailment contact–impact between the car body and railway tracks

Compared with contact–impact interactions between car bodies, the post-derailment contacts between the vehicle and the railway track are more complex and unpredictable. From intermittent abrasions left by tests and accidents [12, 21–26], it can be found that collisions between the motor, brake disc, gearbox, and rail frequently occur since the wheel falls on the railway track in a similar parabolic motion. As shown in Fig. 5, the main post-derailment contact–impact behaviours between vehicle components and railway track are summarized as follows:



Fig. 4 Two typical contact–impact behaviours between the car bodies

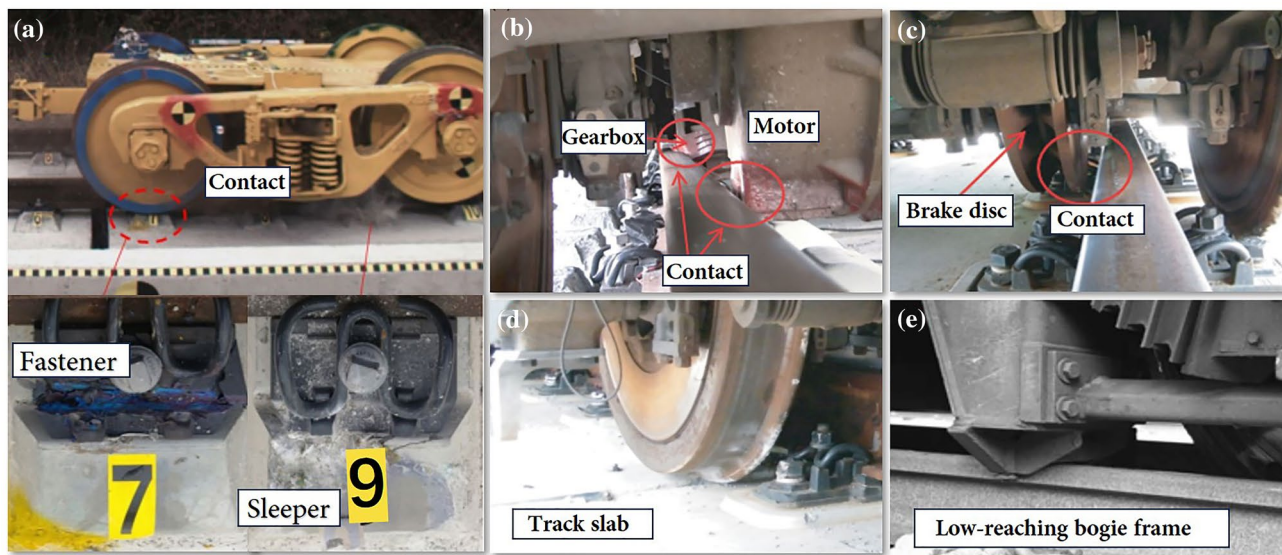


Fig. 5 Typical contact–impact between vehicle components and railway track: **a** wheel–fastener contact and wheel–sleeper contact [27]; **b** rail–gearbox contact and rail–motor contact [12]; **c** rail–brake disc contact [12]; **d** wheel–track slab contact [12]; **e** rail–bogie frame contact [16]

- the contact–impact between the wheel and the sleeper,
- the contact–impact between the wheel and the fastener,
- the contact–impact between the gearbox and the rail,
- the contact–impact between the motor and the rail,
- the contact–impact between the brake disc and the rail,
- the contact–impact between the wheel and the track slab,
- and the contact–impact between the low-reaching bogie frame and the rail.

2.2.3 Post-derailment contact–impact between the vehicle and surrounding structures

In addition to colliding with track structures and other rolling stock, derailed vehicles can also run off the track and collide with nearby structures, such as tunnels, platforms, and buildings. Previous accident scenes have demonstrated that such collisions can cause significant damage or destruction to these structures, as shown in Fig. 6, presenting a serious safety risk to the area. Therefore, it is crucial to consider the safety implications of derailments on nearby structures and implement appropriate measures to protect surrounding buildings and individuals.

2.3 Post-derailment dynamics tests

The most reliable method for analysing and studying the dynamic behaviours of rolling stock is through tests, which mainly include laboratory tests and field tests. In post-derailment studies, laboratory tests typically use scaled models instead of full-scale railway vehicles. While scaled models have advantages such as low cost and ease of operation,

there remains an issue of unclear similarity. For instance, a 1/10 scale vehicle and roller rig were used to examine the derailment process caused by a large earthquake, which could provide a large amplitude excitation condition [28]. However, the analogical work (similarity) was not explained well. Similarly, Cao et al. [22] constructed a scaled model to investigate the response of a train-ballasted track-subgrade system subject to an earthquake, but the reason for selecting scale factors such as geometric dimensions and density was unexplained.

Only a few laboratory full-scale tests were conducted for the wheelset [29] or bogie [30], and not for the full-scale vehicle. Most of these tests were focused on derailment, but they were also useful in understanding post-derailment behaviours, especially the complex wheel–track contact interactions. It is worth noting that laboratory tests were often used to test objects statically, which made it difficult to study the effect of dynamic parameters such as derailment velocity.

For the specific purpose of post-derailment investigations, four major experiments have been conducted since 2011, as summarized in Table 1 [12, 13, 24, 31]. Among the four experiments, the derailment velocity varied from 16 to 60 km/h. Two of them were conducted in the laboratory, and the others were conducted in the field. There are three main purposes of these experiments: (1) to understand the post-derailment behaviours, such as the effect of track type on post-derailment behaviours [12] and hump in the concrete track [13]; (2) to evaluate anti-derailment or vehicle-mounted post-derailment protection devices, such as the stopper [24] and the safety device [12]; and, (3) to verify

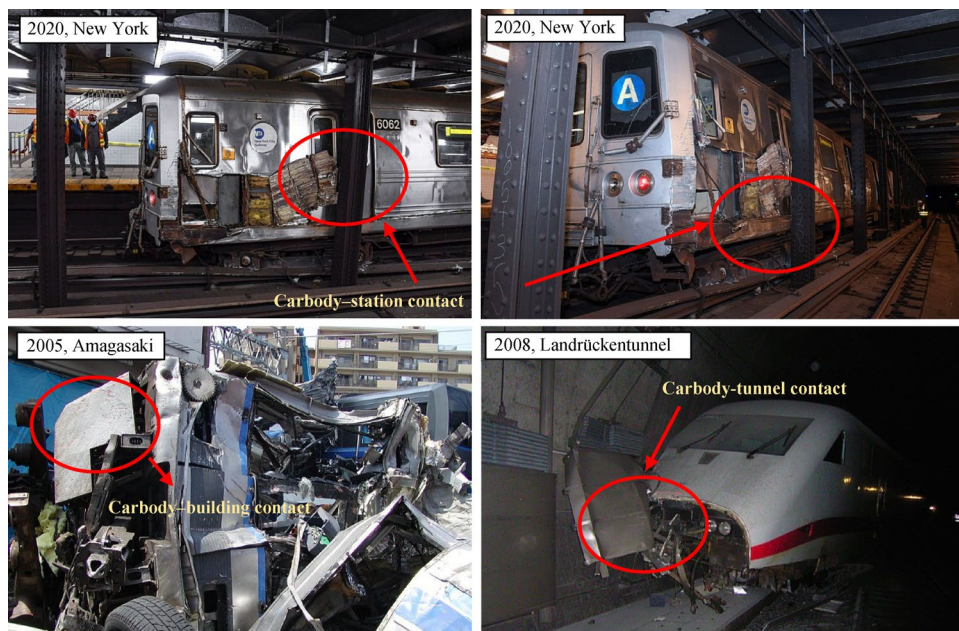


Fig. 6 Typical post-derailment scenarios where a derailed vehicle has impacted surrounding structures, including stations, tunnels, and buildings

Table 1 Four major experiments for post-derailment investigation in recent years

No.	Year	Country	Experiment scenario	Site	Purpose	Derailment velocity (km/h)	Object	Major findings
1	2011	Japan [24]		Laboratory	To develop the stopper and evaluate its efficacy	60.00	Bogie frame equipped with a stopper	Peculiar motions of the bogie frame when the stopper was attached during running tests were observed. Data obtained from the test can be used to calculate static equilibrium conditions of the corresponding simulation model
2	2014	China [31, 32]		Laboratory	To investigate the post-derailment dynamic behaviours and evaluate a developed dynamic model	16.00	Half-car	The continuous collision phenomenon between the gearbox and rail was observed A developed dynamic model was verified by this experiment
3	2016	China [12]		Field	To study the post-derailment safety measures	20.00 30.00	Train equipped post-derailment safety measures	The post-derailment motion of the vehicle mainly consists of the running and the vertical bounce. The gearbox plays an important role in restricting the lateral motions of the derailed motor vehicle. CRTS-II bi-block sleeper ballastless track contributes to constrain the lateral movement
4	2019	Korea [13]		Field	To verify the performance of derailment protection facilities(DCPS)	28.08 55.05	Casting bogie	Humps in the concrete track affected the post-derailment behaviour of the bogie when the derailment velocity was 28.08 km/h. For a higher derailment velocity (55.05 km/h), significant lateral movement of the derailed bogie was observed

the effectiveness of railway track-mounted post-derailment protection facilities, including guard rails [24] and the containment wall [13]. These experiments provided insight into the complex post-derailment behaviours and verified a few newly developed post-derailment protection measures.

The first experiment aimed to evaluate the efficacy of the developed stopper, which caught the guard rails to prevent a derailed vehicle from deviating from the track centreline. The derailment velocity reached 60 km/h in this experiment.

The second experiment revealed the sequence of the wheelset's contact with the rails, fasteners, and sleepers after the derailment, as shown in Fig. 7. The whole process includes three stages: (a) the wheel falls on the fastener, and only collides with the fastener; (b) the wheel continues to move laterally and falls on the sleepers; (c) when the wheel falls on the track slab, the motor collides vertically with the top of the track.

The third experiment found a negative correlation between the vehicle weight and post-derailment distance, contrary to the derailment speed. Increased vehicle weight was associated with decreased lateral displacement after

derailment. Different types of slab tracks were also investigated and compared. The results showed that, compared to the ballastless track slab (CRTS I), the double-block ballastless track slab (CRTS II) had better performance in shortening the post-derailment distance and lateral motion due to its high shoulder.

The fourth experiment was a full-scale and in-field train bogie post-derailment test. The diagram in Fig. 8 shows the typical process of such an experiment [26].

These experiments highlight several aspects that require special attention when conducting train post-derailment experiments, including:

- To obtain sufficient data during the short duration of post-derailment contact, the sampling frequency can be selected from 1000 to 10,000 Hz. For instance, the sampling frequency was set to 5000 Hz in the low-speed running test [12], allowing the detailed recording of the entire post-derailment process.
- To eliminate noise from the raw test data, a filtering process is necessary. The standard EN 15227 (Railway applications—Crashworthiness requirements for railway

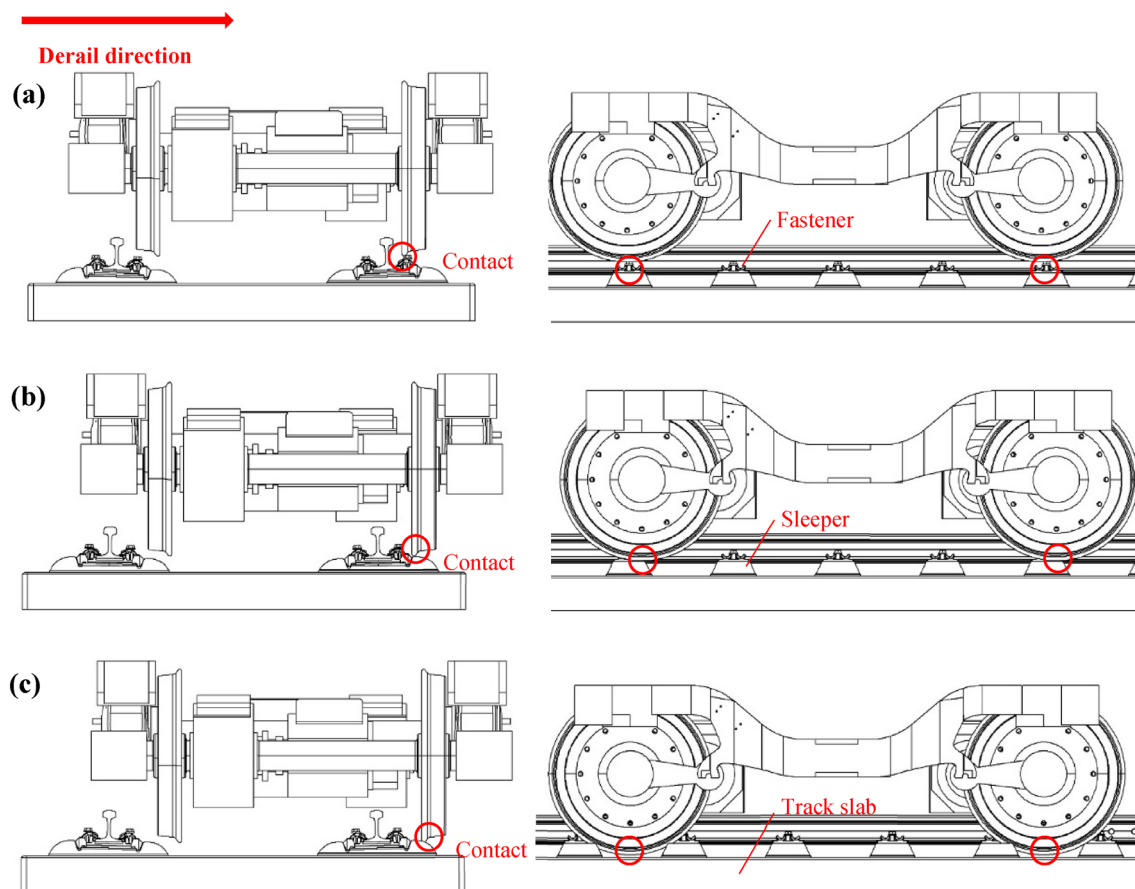


Fig. 7 The post-derailment contact procedure between wheelset and track: **a** contacting with fasteners; **b** contacting with sleepers; **c** contacting with track slabs

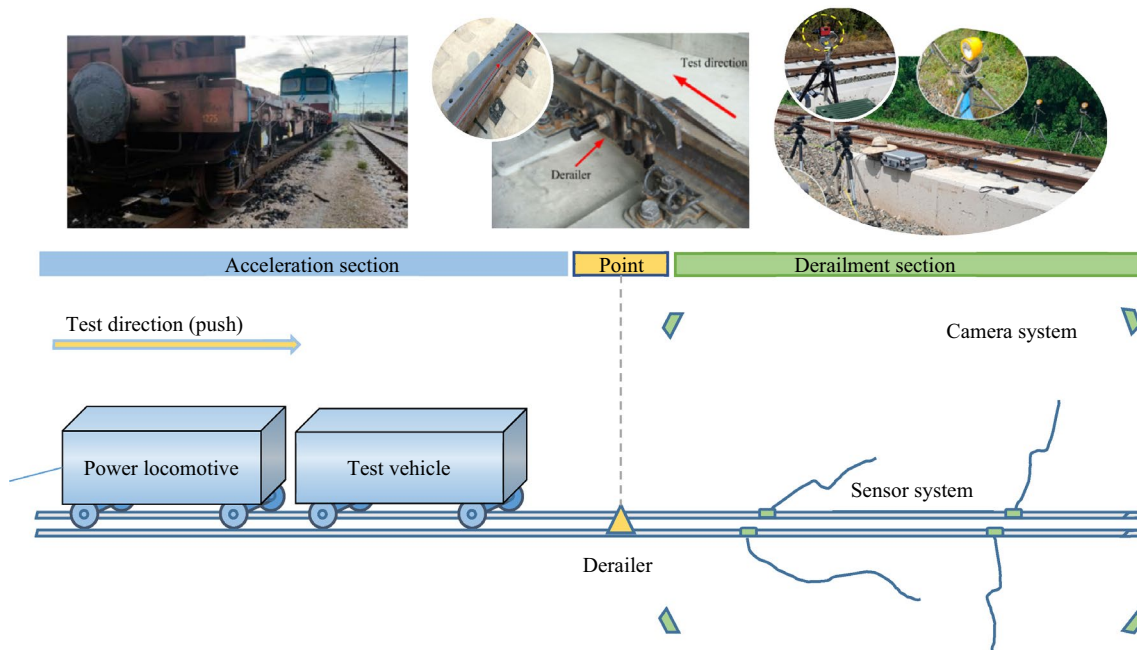


Fig. 8 Typical test apparatus and process of a post-derailment experiment

vehicle bodies [33]) recommends the average method [34] and Butterworth low-pass filtering with 180 Hz.

In summary, the three testing methods have unique advantages and limitations. Laboratory tests with scaled models are more suitable for conducting preliminary research on train post-derailment behaviour due to their ability to generate a large amount of data quickly and at a relatively low cost and easy operation. It can safely and controllably perform difficult-to-repeat tests, such as seismic derailment, by providing high-amplitude excitation. However, accurate consideration of the model similarity ratio is necessary to ensure the accuracy and reliability of test results. Laboratory full-scale tests can replicate and analyse the post-derailment behaviour of full-size wheelsets and bogies, with a short test period, relatively low cost, and adjustable test parameters. However, the scope of post-derailment research is limited by the size of the laboratory. Laboratory full-scale tests are more suitable for evaluating the post-derailment behaviour of a specific vehicle or track under actual size and load. Field tests offer the most accurate representation of post-derailment behaviour for full-scale vehicles or trains under real-world conditions. The limitations of field tests primarily involve high risks and costs, complex data processing, and difficulties in controlling test variables. Therefore, it is crucial to select appropriate test methods according to specific research objectives, resources, and expertise to improve the reliability of experimental and research results.

2.4 Post-derailment dynamics simulation

Due to the high cost and safety hazards of the train post-derailment experiments, numerical simulations have become a popular alternative in this field.

2.4.1 Modelling the post-derailment contact–impact behaviours

After a derailment, the train's movement is guided by complex and ever-changing interactions, as mentioned earlier. These interactions differ from the single pre-derailment wheel–rail interaction that existed before the derailment. To achieve an accurate analysis of train post-derailment behaviours, it is necessary to model the dynamic characterizations of the post-derailment contact behaviours. However, the post-derailment contact behaviours involve a variety of highly nonlinear contact interactions and large elastoplastic deformation, which pose great difficulties and challenges in their dynamics modelling and simulation. Therefore, existing studies generally use a simplified modelling method [18, 19, 35–37].

The process of post-derailment contact–impact modelling typically involves three steps: (1) identifying all possible post-derailment contact–impacts, (2) detecting the occurrence of contacts, contact area or point, and (3) calculating the contact force. An overview of the process of post-derailment contact–impact modelling is shown in Fig. 9.

The detection of contacts and calculation of contact–impact forces are critical to model the contact behaviour

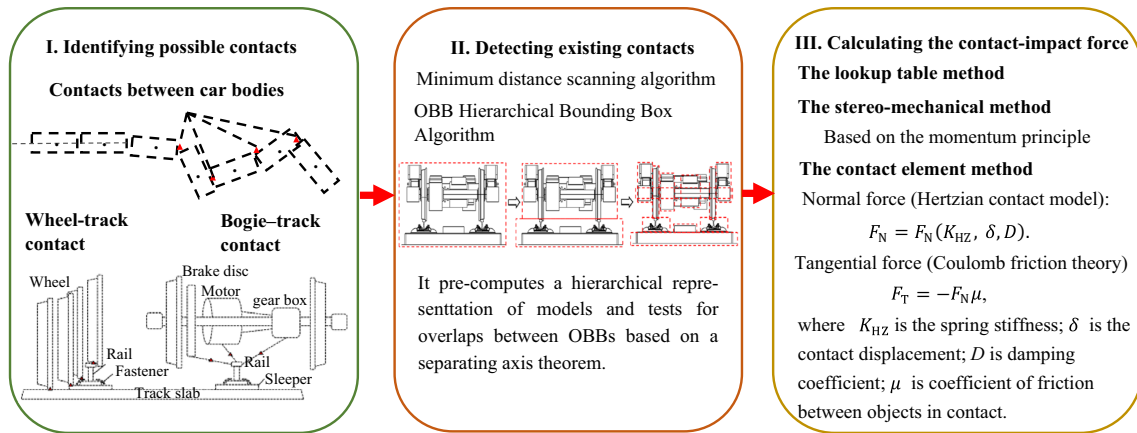


Fig. 9 The process of modelling the post-derailment contact-impact behaviour

between vehicle components and the railway track. Different methods are used to detect contact and calculate contact-impact forces depending on the contact conditions

2.4.1.1 Contact detection When a train derails, its components, such as wheelsets, car body, and bogie frame, make contact with the track components, including rails, fasteners, sleepers, and track slab. Detecting the contact point or location is essential to calculate the contact force accurately. To support the analysis of derailments or switch scenarios, researchers developed a generic wheel-rail contact detection formulation [38] capable of detecting lead and lag flange contact online. In the collision-caused derailment scenario, the minimum distance scanning algorithm was used to detect the contact points between the wheel and the track [39]. Tanabe et al. developed a software (DIASTARS [40]) used to simulate the post-derailment behaviours of the Shinkansen high-speed train caused by an earthquake. To improve contact calculation efficiency, researchers proposed a simple contact detection algorithm that used the displacement between the point on the multi-body system (MBS)

model and the surface on the finite element (FE) model of the railway track [41]. As shown in Fig. 10a, three contact statuses (1, 0, -1) were applied to describe whether the vehicle components contact with the railway track. Inspired by collision detection methods in computer graphics, Wu et al. [31, 37, 42] implemented the oriented bounding boxes tree (OBBTree) algorithm [43], widely used in the game engine of computer animation, to detect the contacts of the train post-derailment models. In the OBBTree algorithm, a hierarchical representation of the vehicle components and track structure needs to be pre-computed, and overlaps between the oriented bounding boxes (OBBs) were tested based on a separating axis theory [44]. As shown in Fig. 10b, when the projection of the distance between the two OBBs on the oblique axis ($\vec{T} \cdot \vec{L}$) was smaller than the sum of the projection of the OBB radius on the oblique axis ($r_A + r_B$), the two objects were considered to be in contact.

The point-surface displacement-based method simplifies the contact object by representing it as a shape composed of sensor points for faster detection. However, its accuracy is heavily dependent on sensor point density, which can lead to

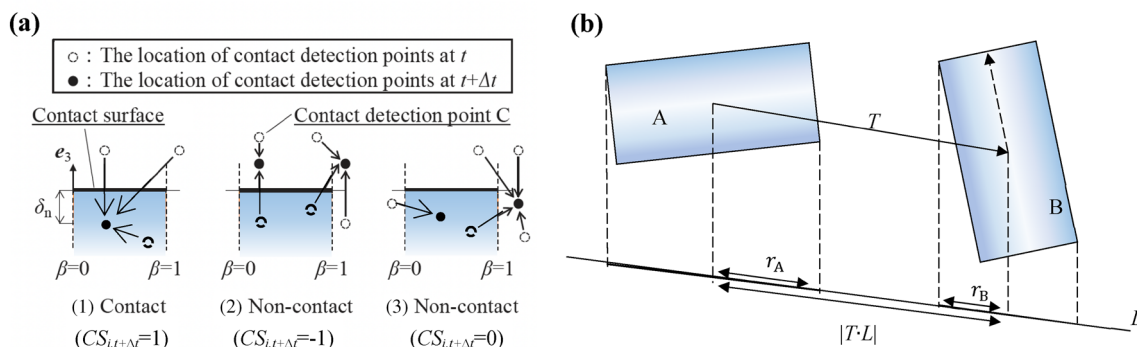


Fig. 10 The methods of determining the contact status: a the point-surface displacement-based method [41]; b the separating axis method [44]. CS is contact status, T is the distance between object A and B, r_A and r_B are the OBB radius on the oblique axis, and L is the separating axis

incomplete detection of non-convex shapes. The minimum distance scanning algorithm can accurately detect dynamic collisions of non-convex bodies. However, it requires multiple scans for complex objects, which significantly increases computational complexity. The OBBTree algorithm has the ability for handling objects of various shapes, but its implementation is intricate and time-consuming. As a result, when choosing an algorithm for a simulation model, it is crucial to consider the pertinent scenarios and specific objectives for its application. For example, the point-surface displacement-based method is well suited for simplified train derailment collision detection, whereas the OBBTree algorithm is appropriate for derailment detection that retains specific structures, such as motors and gearboxes. The minimum distance scanning algorithm is ideal for post-derailment research that requires a certain level of detection accuracy.

2.4.1.2 Contact-impact force calculation The momentum-based technique and the force-based technique are two modelling techniques that have been used in post-derailment investigations of rolling stocks. Post-derailment contact-impact is a highly nonlinear phenomenon, which makes constructing its dynamic model very difficult. The momentum-based technique assumes that the contact is instantaneous and applies the impulse-momentum law to estimate the velocity of the collided rigid body. Although this technique is simple and computationally efficient, it cannot provide information on transient stresses, collisional forces, and impact duration. Due to its simplicity, this technique has been widely used in the early stage of post-derailment investigations for 1D or 2D simulation [16, 45]. The equations for this technique are described as follows:

$$v'_1 = v_1 - (1 + e) \frac{m_2(v_1 - v_2)}{m_1 + m_2}, \quad (1)$$

$$v'_2 = v_2 + (1 + e) \frac{m_1(v_1 - v_2)}{m_1 + m_2}, \quad (2)$$

where v_1 and v_2 are the speeds of the contact objects before contact; m_1 and m_2 are the masses of the contact objects; v'_1 and v'_2 are the speeds after contact; e is the coefficient of restitution.

The momentum-based technique often creates a significant gap with reality. In complex derailment cases, the force-based technique is widely used to compute contact-impact forces following derailments. The force-based technique describes the contact interactions with a force element. Once the contact is detected, the contact force element will be activated. In the early days, piecewise linear springs force elements obtained from FE or experimental data were used to simplify the calculation of contact forces:

$$F_C = K_C(\delta_C), \quad (3)$$

where K_C is the function to describe the relationship between the penetration depth δ_C and the contact force F_C and is obtained from tests or finite element method (FEM) simulations. However, the piecewise linear springs ignore the energy dissipation of the contact.

To simulate energy loss during a collision, the nonlinear spring-damper force element is widely used in the modelling of post-derailment contact-impact behaviour [16, 20, 24, 35, 46, 47]. Normal contact forces are generally represented by the formula that relates to the stiffness and damping coefficient:

$$F_n = K\delta^c + D\dot{\delta}, \quad (4)$$

where K is the stiffness coefficient; δ is the contact depth between contact objects; c is the rigidity index; D is the damping coefficient; $\dot{\delta}$ is the relative velocity between contact objects.

Tangential contact forces are simplified and calculated by using the Coulomb friction model [11, 40, 46, 48, 49]:

$$F_f = \mu F_n, \quad (5)$$

where μ is coefficient of friction.

2.4.2 Typical post-derailment contact-impact models

2.4.2.1 Contact-impact models between car bodies The contact model between car bodies should be considered first since they have a significant influence on the final attitude and posture of the derailed vehicle. Anderson [50] established a contact model between car bodies using the impulse-momentum-based method, which is based on the classical collision theory. There are several assumptions in Anderson's model, such as the time duration of colliding between vehicles being infinitesimal, and the displacement of the car bodies being constant. However, these assumptions do not fully reflect the actual situation of collision between car bodies, which are shell structures rather than

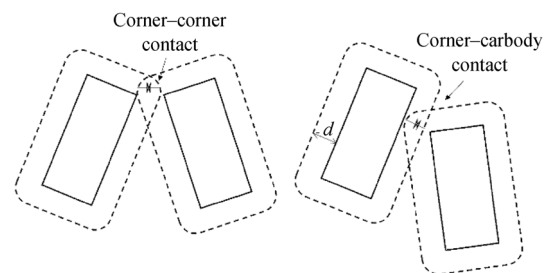


Fig. 11 Contacts of the car bodies. d is the contact depth at maximum damping

solids. A better method to describe the contact between car bodies is the contact force element, which can simulate complex deformations in contact areas and energy dissipation. Both corner-to-corner contact and corner-to-car body contact are modelled as nonlinear force elements, as shown in Fig. 11 [20]. The normal contact force, F_n , is composed of elastic force F_e and damping force F_d .

$$F_n = \begin{cases} 0 & \sigma < 0 \\ \max [0, F_e + F_d] & \sigma \geq 0 \end{cases} \quad (6)$$

$$F_e = K\sigma^e,$$

$$F_d = \dot{\sigma} \cdot \text{step}(\sigma, 0, 0, d, C),$$

where σ is the contact depth, K is the spring stiffness, d is the contact depth at maximum damping, and C is the maximum damping coefficient. The variation of the damping coefficient with contact depth is described by the step function.

However, these 2D contact–impact models between car bodies have limitations and may not be applicable in all scenarios. In 3D contact–impact models between car bodies, the automatic-surface-to-surface contact method is frequently adopted to detect contact and calculate the contact force in FE simulation [27, 51–55]. The nonlinear elastic–plastic spring force element provided by most commercial MBS software has been used to model the contact–impact between vehicle bodies [56–58].

2.4.2.2 Wheel–sleeper contact–impact model A wheel–sleeper impact model was developed by Yu et al. [47] to describe contact interactions between the wheelset and the sleeper in the event of a derailment. The wheel–sleeper impact model was described by a special set of vertical irregularities instead of a wheel–sleeper dynamics model.

The simplified model could simulate the dropping and running behaviour of the wheelset on the sleepers, but the lateral motion was ignored in this model. To predict the wheelset behaviour after impacting concrete sleepers, Brabie et al. [36, 59, 60] proposed a wheel–sleeper impact model. The geometric relationship between the wheel and the sleeper, considering fastener and without considering fastener, was calculated to detect the contact or non-contact status, as shown in Fig. 12.

Once the vertical contact displacement h_z is greater than 0, and the lateral distance $|\Delta x_{fes-w}|$ between the midpoint of the wheel and the sleeper is less than the radius of the wheel, the geometric relationship between the wheel and the sleeper can be regarded as the contact status. The contact force of the wheel–sleeper impact model is obtained by a look-up table, which is previously generated through finite element simulation. Since the look-up table method is based on the results of finite element simulations or tests, it is difficult to apply this method in other models or working conditions.

2.4.2.3 Wheel–fastener contact–impact model A wheel–fastener impact model was also proposed by Brabie et al. [36]. It was similar to the wheel–sleeper impact model in terms of the geometric description and contact detection. The difference was that the wheel–fastener contact was simulated by a spring of piecewise linear stiffness. The spring was used between the wheel and fastener when the contact occurred, which was considered as plastic deformation and failure of the fastener components. The contact force between the wheel and fastener depended on the nonlinear force–displacement characteristics of the spring, as shown in Fig. 13. The parameter of the force–displacement characteristics was determined by comparisons between the actual derailment accident, the Bomansberget accident, and

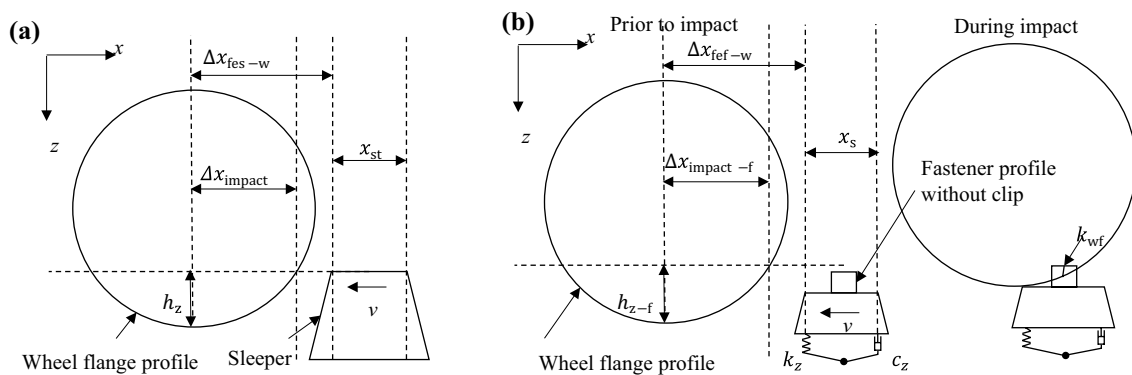


Fig. 12 The geometric relationship between the wheel and the sleeper [36, 59, 60]: **a** without the fastener; **b** considering the fastener. Δx_{fes-w} and Δx_{ref-w} are the longitudinal distances of the wheel lowest point to the sleeper front-edge; Δx_{impact} and $\Delta x_{impact-f}$ are the minimum longitudinal distances at the time of collision; v is the relative speed between the wheel and sleepers; x_{st} and x_s are the longitudinal lengths of sleeper upper surface; h_z is the height between the bottom of wheel and the top of sleeper; h_{z-f} is the height between the bottom of wheel and the top of fastener; k_{wf} is the stiffness coefficient between wheel and fastener; k_z is the stiffness coefficient between sleeper and ground; c_z is the damping coefficient between sleeper and ground

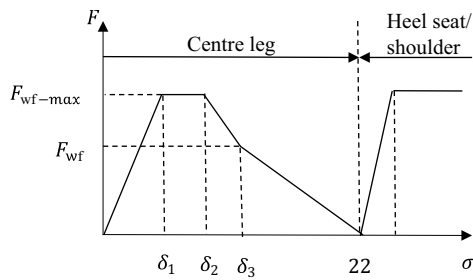


Fig. 13 The nonlinear force–displacement characteristics of the spring for describing the wheel–fastener contact [36]

its MBS simulation counterpart. However, this model possibly generates unrealistic simulation results. For instance, the front wheelset rolled and bounced on the sleepers while the rear wheelset remained on track. Furthermore, some parameters, such as fastener types, track–ground stiffness, and damping, were not considered in the model. At the same time, the longitudinal and lateral force between the wheel and fasteners was ignored.

Based on Barbie’s wheel–fastener impact model, with the assumption of non-deformation in the heel seat and shoulder, Ling et al. [49, 61] proposed a vertical wheel–fastener contact–impact model, which is described by the following equations:

$$F_{wf} = \begin{cases} z_{wf1} \delta & \delta \leq \delta_1 \\ F_{wf-max} & \delta_1 < \delta \leq \delta_2 \\ F_{wf-max} - K_{wf2}(\delta - \delta_2) & \delta_2 < \delta \leq \delta_3 \\ F_{wf-max} - K_{wf2}(\delta_3 - \delta_2) - K_{wf3}(\delta - \delta_3) & \delta_3 < \delta \leq 22 \end{cases}, \quad (7)$$

where δ is the contact deformation between the wheel and centre leg; δ_1 , δ_2 , and δ_3 are average value from brabie’s tests; K_{wf1} , K_{wf2} , and K_{wf3} are the stiffnesses of the centre leg. In addition, the longitudinal and lateral force was described by the coulomb friction law.

2.4.2.4 Motor–guard rail contact–impact model Hironobu et al. [24] proposed a motor-rail (guard rail) impact model to study the motion of motors and a developed stopper between the guard rail during a running test. The contact/non-contact status is determined by the contact force F_n , contact point coordinates z and velocity

$$\begin{aligned} F_n &= (K_{mg}/K_{mg0})F_{n0} - K_{mg}(z - z_0) - C_{mg}\dot{z} - M_g\ddot{z} > 0, \\ z &< \Delta h_m, \\ \dot{z} &< 0, \end{aligned} \quad (8)$$

where K_{mg} and K_{mg0} are the current spring stiffness and initial spring stiffness depending on the longitudinal position of the motor, respectively; C_{mg} is the damping ratio of the

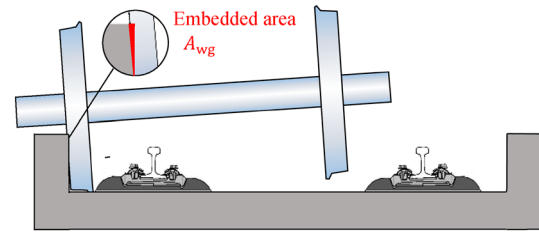


Fig. 14 The wheel–guard contact–impact model [62]

guard; M_g is the mass of the guard; Δh_m is the vertical distance between the contact point of the motor and the guards.

2.4.2.5 Wheel–guard contact–impact model The guard is mounted on high-risk sections of a railway track, to prevent the derailed vehicle from veering off the track. Thus, the direction of the wheel–guard contact–impact force is transverse, as shown in Fig. 14.

The transverse contact–impact force F_T can be calculated by

$$F_T = f_{FP}(P_T), \quad (9)$$

where f_{FP} is the function between the penetration area P_T and the contact–impact force, which is similar to the force–displacement curve of the wheel–sleeper contact–impact force and can be obtained from either FE simulation or experiment.

2.4.2.6 Wheel–track structure contact–impact model A unified model for describing the contact behaviour of wheel and track components, including fastener, sleeper, track slab, etc., was summarized by Ling et al. [49], where the minimum distance scanning algorithm was used to detect whether contact occurred. The contact force f_{nwt} in the vertical direction is defined as a function of the relative displacement between the wheel and the track components, as shown in Eq. (10):

$$f_{nwt} = k_{wt}(u_w - u_t) + c_{wt}(\dot{u}_w - \dot{u}_t), \quad (10)$$

where k_{wt} is the stiffness of the wheel–track structure interaction, which is obtained from a test or FE analysis [63]; c_{wt} is viscous damping; u_w and u_t are the displacement of the wheels and track components in contact, respectively. The tangent forces are described by the coulomb friction theorem, which is related to the sliding friction coefficient μ_{wt} and the relative sliding velocity \dot{u}_{wt} , as shown in Eq. (11):

$$f_{\tau wt} = \mu_{wt} f_{wt} \text{sign}(-\dot{u}_{wt}). \quad (11)$$

This model was applied and validated in several dynamic derailment simulation cases [49, 57, 61, 64]. The

contact surface between the wheel and the track components was assumed to be smooth so that the roughness and damage to the track components were not included in the contact force calculation. To reflect the influence of the surface roughness of track components on the contact force, the multi-point contact model was proposed by Tanabe [40, 62, 63, 65], as shown in Fig. 15.

The contact displacement in the vertical direction between the wheel and track structure in section i is defined as δ_z^i , which is obtained from the displacements of track structure z_T^i , the wheel z_W^i and the roughness of the surface of the track structure in the vertical direction, as shown below:

$$\delta_z^i = z_T^i - z_W^i + \epsilon_z^i \tag{12}$$

The contact force F_z^i in section i is described as a function of the contact displacement δ_z^i :

$$F_z^i = f_C(\delta_z^i), \tag{13}$$

where f_C is a nonlinear function related to the contact displacement. The friction in the transverse direction is defined by the Coulomb friction theorem. Contact checkpoints are set on rigid car bodies to detect the contact between car bodies and FE track structures. The irregularity of the contact surface is considered in the contact displacement calculation. The relationship between the contact force and the contact displacement is obtained by experiments and finite element simulation. However, the effect of the impact velocity and sliding velocity is ignored in the vertical contact force.

A continuous contact force model based on the penalty formulation [66] was adopted by Jun et al. [11] to construct the wheel-track contact-impact model. The model

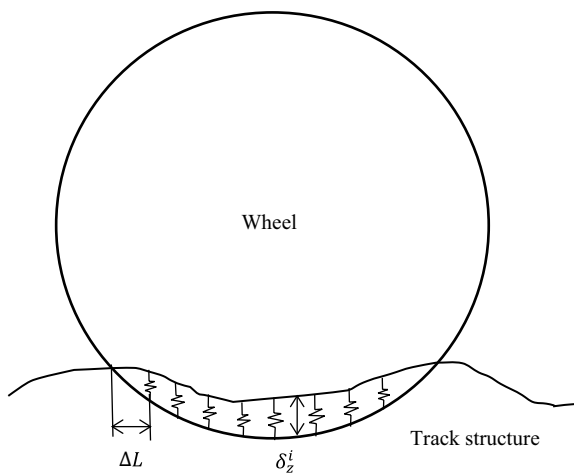


Fig. 15 Multi-point contact spring model [40]. δ_z^i is the displacement of the wheels and track structure in contact, and ΔL is length of each section

considered the geometric characteristics, material properties, friction coefficient, and impact velocity, and derived specific formulas of stiffness coefficient K and damping coefficient D :

$$K = \frac{4}{3\pi(\sigma_1 + \sigma_2)} \left(\frac{r_1 r_2}{r_1 + r_2} \right)^{1/2}, \tag{14}$$

$$D = \frac{3K(1 - c_e^2)}{4v_0'} h^n,$$

where σ_1 and σ_2 are the material properties of the wheel and track related to Poisson's ratio and Young's modulus, respectively; r_1 and r_2 are the radius of the wheel and track, respectively; v_0' is the initial impact velocity; c_e is the restitution coefficient; h is normal penetration depth; n is the expression constant and is set to 1.5.

2.4.2.7 Vehicle-track structure contact-impact model

A vehicle-track components contact model was developed based on the OBBTree algorithm [21], which can model the contact interactions between vehicle components, including the wheel, motor, gearbox, brake disc, and railway track. In the calculation of the normal contact force, Hertzian spring contact theory with hysteretic damping was used, and its formula was shown as follows:

$$F_N = \begin{cases} K_{HZ} \delta^{3/2} \left(1 + \frac{3(1 - \epsilon^2)}{4} \frac{\dot{\delta}}{\delta^{(-)}} \right) & \delta > 0 \\ 0, & \delta \leq 0 \end{cases}, \tag{15}$$

where K_{HZ} is the Hertzian contact stiffness; δ is the contact penetration; ϵ is the collision restitution coefficient; $\dot{\delta}$ is the approach velocity of the two objects at any time; $\delta^{(-)}$ is the relative approach velocity of the two contact objects when they start to contact each other. The tangential force of the collision can be calculated by Coulomb friction force.

The proposed model was integrated into ADAMS/rail by secondary development to avoid computing interruption caused by the failure of the wheel-rail contact force element when the wheel deviated from the rails and kept a long duration.

The typical post-derailment contact-collision models mentioned above utilize various methods, all of which necessitate geometric analysis of the object shape to determine contact. Widely used methods for contact-impact force calculation include the look-up table method, the stereomechanical method, and the contact element method. The general approach is to determine the contact status and compute the relative displacement according to the object geometric relationship, and then calculate the contact force using the formula $f=kx$ (k is the contact stiffness, and x is the contact displacement between contact objects). As

more contact parameters are considered, modified formulas need to be proposed.

2.4.3 Typical post-derailment simulation methods

The 2D simulation model of the train post-derailment dynamics was widely in the early days because of its advantage in the modelling complexity. Yang et al. [17] first proposed the 2D post-derailment dynamics model of a train in 1972. In this model, each vehicle body had only three degrees of freedom. Although the number of derailed vehicles generated by this model matches well with the statistical data from authentic derailment accidents, there was an overlap between vehicles that does not occur in a real accident (Fig. 16a). The reason is that this model was incapable to simulate the coupler failure, uncoupling and collision between vehicles. References [18, 19] addressed these limitations by using stiff springs to represent the couplers. Different from Yang's 3D model, this 4D model can estimate vehicle rollover after derailment, as shown in Fig. 16b. Similarly, to analyse the influence of derailed vehicles on adjacent structures, a 2D equation was used to describe the post-derailment motion [67]. The influence of the derailment velocity, the friction coefficients, and the derailment angle on the post-derailment behaviour were discussed. Edward [20] in Canada used a plane rigid body model to simulate and calculate the resistance of a truck derailment accident. The connection between vehicles was considered in the model, which was regarded as a hinge constraint. It avoided the shortage of stiff springs in the Anderson model, and the results were closer to reality, as shown in Fig. 16b. Additional 2D post-derailment dynamics models can be found in Ref. [46].

In the above works, all models are implemented by self-developed computer programs. With the emergence of commercial simulation software, researchers have begun to build 2D post-derailment dynamics models using commercial multi-body dynamics software, such as ADAMS [46, 68]. The high computational efficiency of commercial software made it easy to conduct a sensitivity analysis of a few parameters including the number of vehicles, the friction coefficient, the characteristics of the coupler (coupler stiffness, length, and maximum swing angle), and the initial condition of the train (angular velocity and longitudinal velocity).

The results show that the derailment speed, the friction coefficient, and the characteristics of the coupler have a great influence on the overall post-derailment motion of the train.

2D simulation of train post-derailment dynamics can tentatively reveal the forces and the interactions among vehicles and surrounding structures under different initial conditions, which has certain significance to understand the train post-derailment behaviour. However, the simplification of contact interactions in the 2D models has dramatically reduced the reliability and accuracy of their simulation results.

Generally, 3D MBS simulation is capable of modelling and simulating all interactions among vehicles and under-track structures during the entire derailment process. Compared with the above 2D models, 3D MBS models have better performance in simulation accuracy, but with a high cost of computation. Therefore, unlike the 2D post-derailment models constructed by self-developed programs, almost all 3D MBS simulation cases of train post-derailment dynamics that we found in the literature use commercial MBS software, such as SIMPACK [58, 69], UM [70], ADAMS [21], MEDYNA [47], DADS [23], and GENSYNS [35, 36].

An MBS model of a train set was built by Han et al. [23] using commercial MBS software DADS to simulate the collision-causing derailment. The MBS model consisted of 20 cars, with the first 5 cars modelled in detail including bogie, suspension element, coupler, and car body, while the remaining 15 were simplified as lumped mass to improve computational efficiency. This MBS model is capable of simulating the overriding and lateral buckling phenomena during and after a train derailment, but improvements are needed to enhance its computational efficiency and simulation capability for large structural deformations.

A comprehensive MBS post-derailment model of the Swedish high-speed tilting train X2000 was developed by using the MBS software GENSYNS for studying its post-derailment dynamic behaviour [35, 36, 60, 71, 72]. The accuracy of the developed MBS models was verified through its FE counterpart simulation in LS-DYNA. By using the developed model, the influence of the train design parameters on the post-derailment behaviours and calculation consequences were analysed in detail.

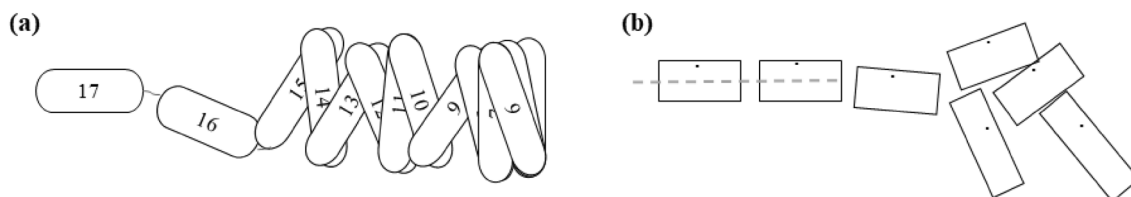


Fig. 16 The results of the 2D post-derailment dynamic simulation: **a** overlap between vehicles generated by the first post-derailment dynamic model developed in 1972 [16, 17]; **b** an improved post-derailment model which can simulate the failure of the couplers [18, 19]

A post-derailment dynamic model of a half-car was established and implemented by the secondary development in ADAMS/rail. But there was no comparison of the difference or similarity between the half-car and the full-scale vehicle in this study [21, 31, 39]. The post-derailment dynamic model was also used to investigate the post-derailment behaviour of a high-speed train set consisting of two motor cars and two trailer cars [37].

An MBS truck–train collision model was proposed by Ling [39], in which the truck was modelled as a nonlinear mass-spring system, while the train was described in derailed MBS model with 42 DOFs in each vehicle. A 3D train–track dynamic model [73] based on the vehicle-track dynamics model was developed to verify the protective effect of guard rail on a derailed freight train and the surrounding environment [11]. This model was composed of 4 subsystems, including a vehicle system, track system, wheel–rail contact system, and coupler buffer system. The post-derailment dynamics model was compared with a pre-derailment dynamic model to validate its validity.

Although the MBS-based post-derailment model has the advantages of predicting the gross motion of a train set, fast modelling, and high computational efficiency, it cannot simulate the large deformation when the high-speed impact occurs after a train derails and directly analyse the stress/strain of the contact object. In contrast, FE simulation can clearly reflect the elastic–plastic behaviour and energy dissipation between colliders after the derailment, providing better simulation accuracy.

A simplified FE bogie model was proposed by Song et al. [27, 74] to investigate the train post-derailment behaviours. Instead of constructing the detailed FE bogie model, a node with mass and moment of inertia of the bogie frame was placed at the centre of gravity of the bogie. The reason for simplifying the bogie was that the author assumed that the simplified parts of the bogie will not contact the railway track after the train derailed. This simplification reduced the number of elements from about 80,000 to 1, as shown in Fig. 17, which dramatically decreased the scale of the FE model, and largely improved the solving efficiency.

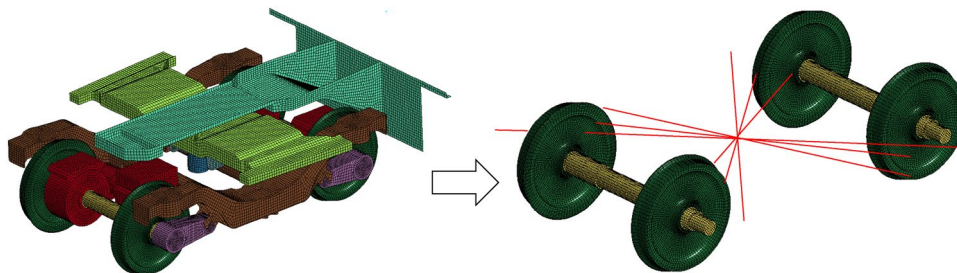


Fig. 17 The simplified FE bogie model for the train post-derailment study [27, 73]

However, simplified FE models usually lead to the loss of simulation accuracy. The FEM–MBS co-simulation method, which combines the advantages of both MBS and FE, has become a dominant method for post-derailment simulation in recent years. One of the combined methods is that the nonlinear characteristics obtained from the FE simulation are integrated into the MBS model as a force element, which was used in an early stage of post-derailment studies. For example, Brabie [36] developed a FE wheel–sleeper model to generate a look-up table which was used in the MBS post-derailment model to calculate the contact force between the wheel and the sleeper.

Another method for combining FE and MBS in the post-derailment study is to use force elements to directly integrate the MBS model with the FE model. This method was proposed by Tanabe et al. [40, 62, 63, 65] to study the post-derailment dynamic behaviours of the Shinkansen train caused by an earthquake. The train and the railway structure were constructed as a MBS model and an FE model, respectively, and a multi-point contact springs model was used to combine the two models. In addition, a modal reduction method and a robust time integration method were applied to reduce the solving time and improve the stability of the combined model, respectively. Based on Tanabe's method, a combined FE–MBS 3D train–track–bridge model was developed by Ling et al. [39] to predict the post-derailment behaviour of derailed trains on the bridge. FE modal analysis was used to determine the mass stiffness matrix of the bridge, and the train–track–bridge dynamic equation was established. To efficiently compute the nonlinear equations generated by the numerical model, an explicit integral algorithm based on the Newmark method, which is proposed by Zhai [73, 74], was used to solve these equations.

3 Containment methods of post-derailment behaviours

The aim of understanding the post-derailment behaviours of rolling stock is to find a solution for restraining the derailed vehicle deviated from the track centreline too

far, and consequently guiding and stopping a train after a derailment in a much safer way, instead of the wheel–rail interaction. Substitute guidance mechanisms (SGMs) are exactly used for achieving such a purpose. They are devices or facilities mounted on vehicles, railways, or components of a vehicle itself to guide the running train. As a railway-specific passive safety protection and accident prevention method, it is proved that SGM can efficiently diminish the severity of a derailment accident. SGMs can be roughly divided into three types, as shown in Fig. 18.

- Vehicle component-based SGM (indicated in green in Fig. 16). Purpose-designed vehicle components act as an SGM, such as the brake disc, bogie frames, and gearbox [21].

- Vehicle-mounted SGM (indicated in pink in Fig. 16). Specific devices are mounted in the vehicle for anti-derailment or derailment escalating containment. A typical example is the ‘L-shaped guide’ device in Japan [7].
- Railway track-mounted SGM (indicated in yellow in Fig. 16). The guiding facilities are installed in or along the railway track, such as guard rail, restraining rail, and various types of derailment containment provision (DCPs) [9].

3.1 Vehicle component-based SGMs

Past derailment accidents [71] and laboratory [12, 31] and field tests [13] have shown that certain components of a vehicle, such as brake discs, gearboxes, and low-reaching

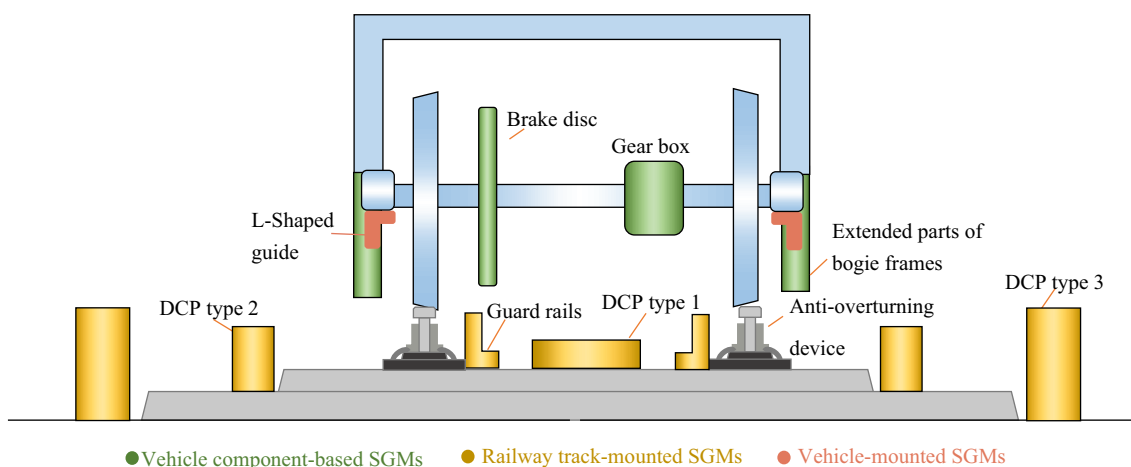


Fig. 18 Three types of SGMs

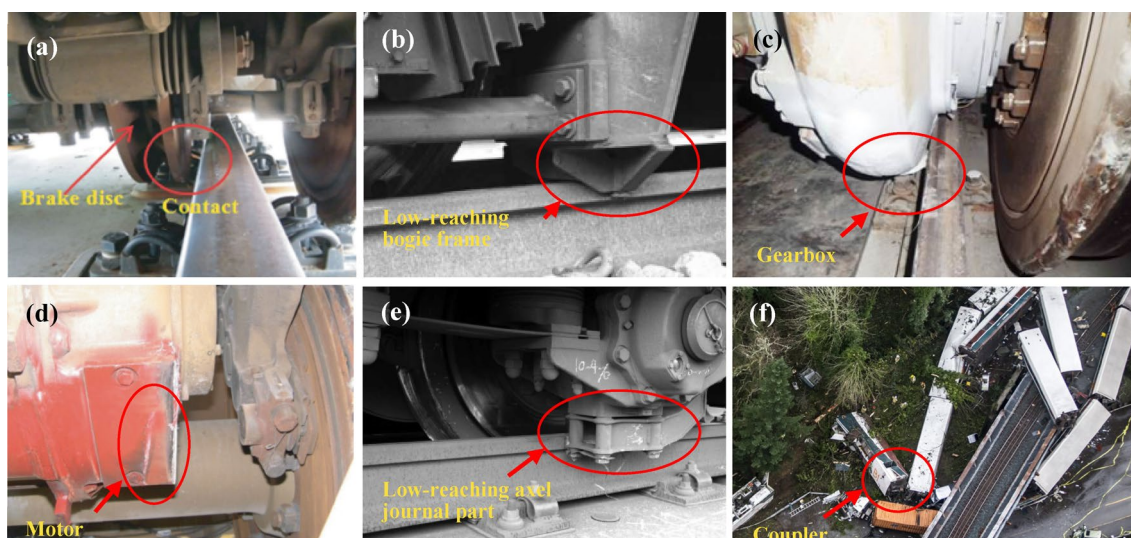


Fig. 19 Typical vehicle component-based SGMs: a brake disc [12]; b low-reaching bogie frame [71]; c gearbox [31]; d motor [12]; e low-reaching axel journal part [71]; f coupler

bogie frames, can guide a derailed vehicle to a safe stop. Some of the vehicle component-based SGMs are illustrated in Fig. 19.

As shown in Fig. 19, the low-reaching bogie frame and axle-mounted parts, including the low-reaching axle journal, gearbox, and brake disc, have the potential to serve as SGMs [16]. The guidance condition is created when the rails fill into the lateral gap between the SGMs and the wheel. Lateral derailment velocity impacts the effect of minimizing the lateral displacement of the SGMs. Within a lateral derailment velocity of 1.7 m/s, the lateral impact force generated by the contact and collision between the vehicle component-based SGMs (brake disc, gearbox, low-reaching part) and the rails is enough to keep the vehicle staying on track. By contrast, when the lateral velocity of derailment is greater than 1.7 m/s, these components cross over the track under the combined action of the vertical displacement produced by the wheels bouncing from the sleepers and the lateral displacement produced by the lateral motion of the car body, in this case, the derailed vehicle cannot be stopped by the vehicle component-based SGMs [24].

Motors have a smaller guidance ability compared to the low-reaching bogie frame and axle-mounted parts due to their different contact status [22–24]. When a derailment occurs, the motor generally collides with the top of the rail in the vertical direction, and sometimes slides. It cannot help limiting the lateral displacement of a derailed vehicle. However, the friction between the bottom of the motor and the top of the rail can play a positive role in reducing lateral deviation. This is because the motor is positioned higher above the rail than the brake disc and gearbox, which prevents it from making lateral contact with the rail.

Other vehicle components including the coupler (maximum rotation angle and coupler height) and wheel flange have also the potential to reduce derailment consequences [7, 13]. The coupler can be the ultimate barrier to avoid lateral deviations after a derailment. If the stiffness is robust enough, the adjacent vehicle would not be revolved extremely [19]. The wheel flange will be constrained between the rails and shoulders during the derailment, leading to a restriction on the lateral movement of the vehicle.

In addition, a special wheelset is designed and proved that adding additional running area and reverse flanges is effective in preventing derailment [7].

The main way to enhance the guidance ability of vehicle component-based SGMs is to increase the possibility of contact or collision between the vehicle components and the track by optimizing their geometry shapes, size, materials, and positions, hence reducing or limiting the lateral offset of the vehicle body.

3.2 Vehicle-mounted SGMs

Unlike vehicle component-based SGM, vehicle-mounted SGMs are anti-derailment devices attached to the vehicle for guiding a derailed vehicle. The position where they are mounted can be in the axle box, bogie frame, etc. The existing vehicle-mounted SGMs mainly include the L-shaped guide [7], the post-derailment stopper [24] developed by Japan, and the post-derailment safety device developed by China [12, 21], as shown in Fig. 20.

The L-shaped guide and the post-derailment safety device are mounted at the axle box, but the post-derailment stopper is attached to the bogie frame to fit the specific track structure of the Tokaido Shinkansen. All three vehicle-mounted SGMs guide or stop the derailed vehicle by resisting its lateral motion, but they are different in the way to prevent lateral deviation. The L-shaped guide and the post-derailment safety device catch on the rails, while the post-derailment stopper catches the guard rail. The L-shaped guide is successfully installed on the in-service trains of running on Tohoku, Joetsu, and Nagano Shinkansen. When the wheelset is derailed, the vehicle-mounted SGMs will contact and rub against the side of the rail or guard, limiting further lateral displacement, as shown in Fig. 20a.

The laboratory test of the vehicle-mounted SGMs verified their validity in low-speed conditions [26]. In addition, the test also clarified that running and vertical bouncing motions are the main component of the post-derailment motion. However, the existing studies only focus on the limitation of lateral motion without considering other directions. Therefore, optimizing vehicle-mounted SGMs with

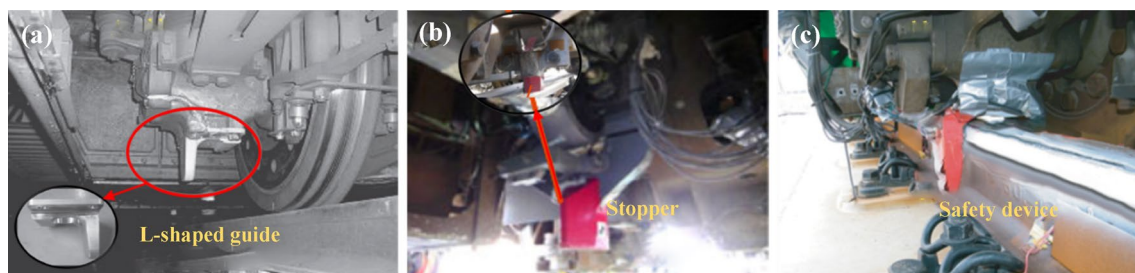


Fig. 20 Vehicle-mounted SGMs: **a** L-shaped guide, Japan [7]; **b** post-derailment stopper, Japan [24]; **c** post-derailment safety device, China [12]

the consideration of multi-directional coupling control needs further study. For example, adding a hook-shaped structure to the L-shaped vehicle-mounted SGM can help collide with the bottom of the rail head vertically, which reduces the kinetic energy of the derailed vehicle.

In addition, the collision between the wheelset and the fasteners causes the failure of fasteners after the derailment, and the force generated by the collision between the vehicle-mounted SGMs and the track may cause the rail to tip over. Therefore, anti-rail overturning measures are often used to prevent the track from overturning when vehicle-mounted SGMs work, such as reinforcing the material stiffness of the fastener and installing protective devices on the rail web.

3.3 Railway track-mounted SGMs

Railway track-mounted SGMs here refer to the DCPs [9] which are usually mounted in high-risk sections of the track, such as sharply curved track sections, bridges, and areas with a high risk of natural hazards (earthquake, landslide, etc.), to guide or stop the derailed train, reduce the severity of a derailment accident, and prevent the secondary damage to the railway infrastructure. Reference [9] divides railway track-mounted SGMs into three types: DCP type 1, DCP type 2, and DCP type 3, as listed in Table 2. DCP type 1 generally use the check rails to keep the rolling stock in line with the subgrade, which is suitable for being applied on the viaduct. The provisions are installed inside the running rails. Different from DCP type 1, DCP type 2 is to place the provisions outside the running rails and applied in locations where it is difficult to use DCP type 1 due to the inside provisions. Like DCP type 2, DCP type 3 is made of a guide wall which is mounted outside of the running rail. The difference in the guide wall is higher and stronger than the guide rails used in DCP type 2. Therefore, the DCP type 3 can provide effective containment ability for a train running at 200–300 km/h.

In Japan, due to the 2004 derailment accident caused by the Niigata Chuetsu Earthquake, the development and study of new passive safety protection facilities have been widely endorsed and supported. For example, a vehicle guide wall equipped on the ballasted ladder track was developed by Kiyoshi ASANUMA [76]. The reinforced concrete wall is mounted outside the track gauge, so a derailment prevention

guard could be placed inside the gauge, further improving the protection ability during the earthquake-caused derailment accident.

Two types of protection facilities in South Korea, guide rails and derailment containment walls, are frequently used in high-speed railway lines [13, 54], as shown in Fig. 21. Guard rails are employed at sharp curves, bridges, and switches. Derailment containment walls are applied on bridges for high-speed railways where the passing speed is over 200 km/h and installed at a relatively long distance from the running rails. The height of the walls is high so that the walls can contact and collide with the sides of the bearing axle box of the bogie when the train has an excessive lateral motion. To evaluate the containment effect of the derailment containment walls, a few simulations [27, 77] and full-scale tests [13] were conducted to analyse the impact force and containment effect in various installation situations.

Taking the guard rail as the representative of the inter-rail device, when the lateral impact derailment occurred [69], the wheels made multiple impacts with the guard rail, and the energy of the whole collision process was consumed by the wheel/rail friction, the wheel/guard rail friction, and the vehicle damper. In the sensitivity analysis of the guard rail, the installation position of the guard rail (the lateral width [58] and vertical heights of the guard rail and the rail), the material properties (friction coefficient, material strength, etc.) and the installation method (fasteners, etc. [70]) have inter-related effects on the performance of the guard rail [13, 78].

3.4 Comparison and analysis of the SGMs

Effective containment methods are crucial for minimizing the risks and consequences of a derailment. Each of the three typical SGMs designed to control post-derailment behaviour has its own strengths and limitations.

Vehicle component-based SGMs are integral to the train's assembly and do not require additional equipment or installation. However, they serve only as auxiliary measures to

Table 2 Three types of DCPS

Type	Collision position	Installed location	Being effective at high speed
DCP type 1	Wheel	Inside the gauge	Not
DCP type 2	Wheel	Outside the gauge	Not
DCP type 3	Bogie	Outside the gauge	Yes

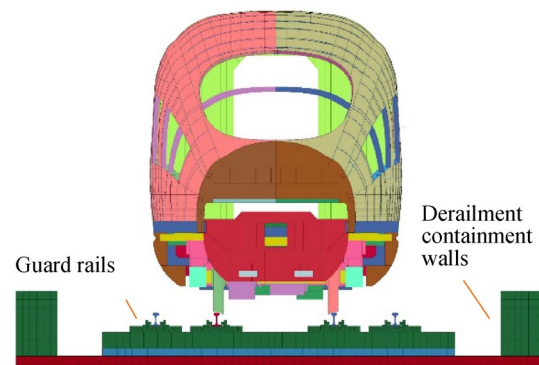


Fig. 21 Guard rails and derailment containment walls used in South Korea

prevent derailment and are effective within a specific speed range. Derailment at high speeds may cause the vehicle to overturn, leading to more severe consequences. Vehicle-mounted SGMs offer superior versatility and flexibility, making them easy to integrate into various trains. Nevertheless, these systems have speed range limitations and require periodic inspections. Therefore, they are most suitable for prolonged operations or in harsh environmental conditions. Railway track-mounted SGMs are highly effective in preventing derailment, but their high construction costs make them feasible only for short-distance track areas such as viaducts and valleys.

In Table 3, we summarize the advantages and disadvantages of the three SGMs to help researchers and decision-makers make informed choices when selecting appropriate containment methods.

4 Future research

Although there is a general agreement on the significance of post-derailment research in improving and enhancing railway passive safety protection, there are still a few arguments and unsolved challenges. For example, there is no unified standard for applying post-derailment containment methods and facilities, and different countries have different solutions. More importantly, these solutions still lack theoretical foundations and thoughtful analysis to support them, such as quantified risk assessment. In addition, the details of the existing methods need to be investigated and further improved, such as real-time dynamics simulations, full-scale field tests, and more refined contact modelling methods. Moreover, the absence of validation experiments for theoretical models of train post-derailment dynamics poses a significant challenge in comprehending the role of post-derailment behaviours in catastrophic derailment accidents. Therefore, to address the above challenges, it is necessary to further ascertain the post-derailment dynamic behaviour and optimize derailment prevention in the future.

Some practicable future research topics listed below are suggested from the following three aspects.

4.1 Post-derailment behaviour modelling

A dynamic model with the ability to simulate the behaviour of both pre-derailment and post-derailment is essential for train post-derailment investigations. However, post-derailment behaviours involve a variety of highly nonlinear contact–impact interactions and large elastoplastic deformation, which pose huge challenges in their dynamics modelling and simulation. In order to establish an accurate dynamic model and predict the post-derailment behaviours of rolling stock, more factors need to be considered. For example, due to the effect of penetration depth, the contact force between the car body and the railway structure is strongly nonlinear and profoundly different from the behaviours assumed by the Hertz law. However, most of the existing contact force dynamic models adopt the simplified Hertz spring–damper model. Therefore, a more accurate contact–impact force model between the car body and the railway structure needs to be further developed as a non-Hertz problem.

On the other hand, computational efficiency is a critical factor to determine the practicability of a contact force model. The existing MBS or FE model has relatively low computational efficiency. Although parallel computing shows great capabilities in improving the efficiency of conventional FEM and MBS simulations, its reliance on high-performance computers significantly inflates the expenses associated with simulation hardware. Therefore, it is worth exploring new alternative approaches that can deliver high computational efficiency while maintaining a reasonable cost level. Therefore, it is worth exploring new methods that can achieve high computational efficiency as well as a reasonable level of accuracy. The physics engine can approximately simulate the dynamic behaviours of objects in the real world based on physical principles, which have been successfully applied in the field of virtual reality, mechanical simulations, vehicle dynamics [52], and other sectors. More notably, the

Table 3 The advantages and disadvantages of the three SGMs

Type	Specific facilities	Advantages	Disadvantages	Application
Vehicle component-based SGMs	Brake disc, bogie frame, gearbox, motor, axle journal part; coupler et al	No additional equipment or installation, easy maintenance	The anti-derailment effect is limited	As an aid to prevent derailment
Vehicle-mounted SGMs	L-shaped guide, post-derailment stopper, and post-derailment safety device	High adaptability and flexibility, easy installation	Speed limitation and periodic maintenance	Long railway section and harsh climatic environment
Railway track-mounted SGMs	DCP type 1, DCP type 2, and DCP type 3	Effective derailment prevention capabilities, and easy maintenance	High installation cost and narrow applicability	Mountainous section, viaduct section, and railway crossing section

collision detection algorithms, which have already been successfully used in the simulation of post-derailment behaviour [21], and the real-time rigid body simulation framework in the physics engine, are suitable for rapidly constructing and simulating the large-scale post-derailment model of a train set. A tentative study of using a physics engine to simulate the train running behaviour has been conducted in [79], which has proved the feasibility of using a physics engine in the dynamic simulation of railway vehicles to some extent. It is also noteworthy that the accuracy of the physics engine-based simulation is inadequate. Therefore, combining physics engine and data-driven simulation methods [80, 81] is more feasible to obtain a reasonable result.

4.2 The adverse effect of the SGMs

There is no doubt that SGMs can help to prevent derailment escalation, thereby reducing the likelihood of severe off-track derailment accidents. The question is whether there are any adverse effects and how they manifest under different conditions and situations. To date, several studies provide some insight into how SGMs work in a derailment process, but these studies focus on specific conditions, and it is not clear whether these SGMs are robust or have adverse effects on the safety of a running train. For instance, almost all existing studies report that SGMs limit the lateral motion of a derailed vehicle. However, vertical and longitudinal displacements also have a significant influence on the train's post-derailment behaviours, especially when the vehicle overturns and telescopes. Therefore, it is crucial to consider the coupling effect of lateral, vertical, and longitudinal motions on the train's post-derailment behaviours. Furthermore, the details of known SGMs require further explorations, such as geometric dimensions, material strength, and installation location, which significantly impact SGMs' containment ability and service life.

Meanwhile, the drawbacks and adverse effects of SGMs require further investigation. Some are understandable, such as additional costs and maintenance, but some need clarification. For instance, whether SGMs may pose additional risks. Fragmented analysis and information already indicate that some SGMs can cause derailment escalation under specific circumstances [9]. An example is the application of DCP type 1. The check rail of DCP type 1 may increase the probability of wheel climb if debris stays between the running rails. Additionally, the check rail also limits the design of the bogie and axle. Therefore, the detailed adverse effects of SGMs need to be specified and identified further. Meanwhile, to address these adverse effects, the optimization of existing SGMs needs to be studied.

In addition, post-derailment protection facilities for railway transportation have been tentatively used in some countries, but their validity, cost–benefit ratio, and

effectiveness have not been well investigated. To improve safety and reduce potential catastrophic accidents, it is urgent to develop more efficient and low-cost facilities for passive safety protection in railway transportation.

4.3 Standardization of post-derailment containment

Almost all existing practical applications of post-derailment containment have been conducted on a case-by-case basis. There is no unified standard or approach that can be used as a reference or recommendation in the study of post-derailment containment. Therefore, promoting the standardization of post-derailment containment, including the design of SGMs, can greatly improve the safety of the railway system.

5 Conclusion

This paper provides a comprehensive review and discussion of existing knowledge and findings related to train post-derailment behaviours and current practical applications of post-derailment containment methods for rolling stock. Understanding post-derailment behaviours is crucial for improving railway passive safety. In recent decades, numerous simulation methods based on FEM and MBS, as well as various practical tests conducted in laboratories or fields, have been proposed and developed. Some of these methods have been widely used in train post-derailment investigations. Our review summarizes key technical points of laboratory and field tests of train post-derailment behaviour and systematically sorts out the widely used FEM and MBS in post-derailment simulation, including post-behaviour contact modelling. We also introduce and analyse the concepts, methods, and applications of SGM-based containment methods for train post-derailment behaviours. Finally, we propose the potential application of artificial intelligence and physical engines in future studies to improve the understanding of train post-derailment behaviours, thereby enhancing railway passive safety.

Acknowledgements The authors gratefully acknowledge the support from the National Natural Science Foundation of China (No. 52172407 and No. U19A20110) and the Natural Science Foundation of Sichuan Province (No. 2022NSFSC0415).

Open Access This article is licensed under a Creative Commons Attribution 4.0 International License, which permits use, sharing, adaptation, distribution and reproduction in any medium or format, as long as you give appropriate credit to the original author(s) and the source, provide a link to the Creative Commons licence, and indicate if changes were made. The images or other third party material in this article are included in the article's Creative Commons licence, unless indicated

otherwise in a credit line to the material. If material is not included in the article's Creative Commons licence and your intended use is not permitted by statutory regulation or exceeds the permitted use, you will need to obtain permission directly from the copyright holder. To view a copy of this licence, visit <http://creativecommons.org/licenses/by/4.0/>.

References:

- Cao Y, An Y, Su S et al (2022) A statistical study of railway safety in China and Japan 1990–2020. *Accid Anal Prev* 175:106764
- Evans AW (2021) Fatal train accidents on Europe's railways: An update to 2019. *Accid Anal Prev* 158:106182
- Liu X, Rapik Saat M, Barkan CPL (2017) Freight-train derailment rates for railroad safety and risk analysis. *Accid Anal Prev* 98:1–9
- Federal Railroad Administration (2020) Train accident reports.
- European Union Agency for Railways (2022) Report on railway safety and interoperability in the EU
- International Union of Railways (2021) UIC safety report 2021—significant accidents 2020—public report
- Kajitani Y, Kato H, Asano K (2010) Development of an L-shaped guide to prevent deviation from rails. *JR East Tech Rev* 15(1):53–56
- Liu X, Barkan CPL, Saat MR (2011) Analysis of derailments by accident cause: evaluating railroad track upgrades to reduce transportation risk. *Transp Res Rec* 2261(1):178–185
- Hamilton BA (2004) Report on the findings of: current practice and effectiveness of derailment containment provisions on high speed lines. HSL-Zuid Organisation, Zoetermeer
- Kuzuta M, Ueki K, Miyamoto T et al (2013) Numerical dynamic simulation of a train set running on ballasted track after derailment. *Q Rep RTRI* 54(2):112–117
- Lai J, Xu J, Wang P et al (2021) Numerical investigation on the dynamic behaviour of derailed railway vehicles protected by guard rail. *Veh Syst Dyn* 59(12):1803–1824
- Guo L, Wang K, Lin J et al (2016) Study of the post-derailment safety measures on low-speed derailment tests. *Veh Syst Dyn* 54(7):943–962
- Bae HU, Moon J, Lim SJ et al (2020) Full-scale train derailment testing and analysis of post-derailment behavior of casting bogie. *Appl Sci* 10(1):59–78
- Schafer DH, Barkan CPL (2008) Relationship between train length and accident causes and rates. *Transp Res Rec* 2043(1):73–82
- Eboli L, Forciniti C, Mazzulla G (2020) Factors influencing accident severity: an analysis by road accident type. *Transp Res Procedia* 47:449–456
- Yang T, Manos W, Johnstone B (1972) A study continuation of derailment behavior final report (phase 08 report on computer derailment study). Railroad tank car safety research and test project. Association of American Railroads, Washington DC
- Yang T, Manos W, Johnstone B (1972). Dynamic analysis of train derailments. In: ASME winter annual meeting, New York
- Birk A, Anderson R, Coppens A (1990) A computer simulation of a derailment accident: part II-sample simulation. *J Hazard Mater* 25(1–2):149–165
- Birk A, Anderson R, Coppens A (1990) A computer simulation of a derailment accident: part I-model Basis. *J Hazard Mater* 25(1–2):121–147
- Toma EE (2000). A computer model of a train derailment. Dissertation, Queen's University,
- Wu X, Chi M, Gao H et al (2016) The study of post-derailment measures to limit the extent of a derailment. *Proc Inst Mech Eng Part F J Rail Rapid Transit* 230(1):64–76
- Cao L, Yang C, Zhang J (2020) Derailment behaviors of the train-ballasted track-subgrade system subjected to earthquake using shaking table. *KSCE J Civ Eng* 24(10):2949–2960
- Han H-S, Koo J-S (2003) Simulation of train crashes in three dimensions. *Veh Syst Dyn* 40(6):435–450
- Sunami H, Morimura T, Terumichi Y et al (2012) Model for analysis of bogie frame motion under derailment conditions based on full-scale running tests. *Multibody Syst Dyn* 27(3):321–349
- Zhao H, Xu P, Li B et al (2021) Full-scale train-to-train impact test and multi-body dynamic simulation analysis. *Machines* 9(11):297
- Diana G, Sabbioni E, Somaschini C et al (2021) Full-scale derailment tests on freight wagons. *Veh Syst Dyn* 60(6):1–18
- Song IH, Kim JW, Koo JS et al (2020) Modeling and simulation of collision-causing derailment to design the derailment containment provision using a simplified vehicle model. *Appl Sci* 10(1):118
- Nishimura K, Terumichi Y, Morimura T, Fukada J (2010) Experimental study on the vehicle safety by earthquake track excitation with 1/10 scale vehicle and roller rig. *J Sys Des Dyn* 4(1):226–238
- Braghin F, Bruni S, Giorgio D (2006) Experimental and numerical investigation on the derailment of a railway wheelset with solid axle. *Veh Syst Dyn* 44(4):305–325
- Miyamoto T, Nobuyuki M, Masamichi S et al (2004) Railway vehicle dynamic behavior against large-amplitude track vibration. *Q Rep RTRI* 45:111–115
- Wu X, Chi M, Gao H (2014) The study of post-derailment dynamic behavior of railway vehicle based on running tests. *Eng Fail Anal* 44:382–399
- Zhai W, Wang K, Liu P et al (2011) Full-scale derailing principle test stand with steering frame operating on rails, CN Patent ZL101995340B (in Chinese)
- Comite European de Normalisation (2008) Railway applications—crashworthiness requirements for railway vehicle bodies (EN15227 B)
- Beason WL, Hirsch TJ, Campise WL (1989) Measurement of heavy vehicle impact forces and inertia properties final report. . Department of Transportation, Washington DC
- Brabie D, Andersson E (2006) Dynamic simulation of derailments and its consequences. *Veh Syst Dyn* 44(sup1):652–662
- Brabie D, Andersson E (2008) Post-derailment dynamic simulation of rail vehicles—methodology and applications. *Veh Syst Dyn* 46(sup1):289–300
- Wu X, Chi M, Gao H (2016) Post-derailment dynamic behaviour of a high-speed train under earthquake excitations. *Eng Fail Anal* 64:97–110
- Pombo J, Ambrósio J, Miguel S (2007) A new wheel–rail contact model for railway dynamics. *Veh Syst Dyn* 45(2):165–189
- Liang L, Dhanasekar M, Thambiratnam D et al (2016) Lateral impact derailment mechanisms, simulation and analysis. *Int J Impact Eng* 94:36–49
- Tanabe M, Goto K, Watanabe T et al (2017) A simple and efficient numerical model for dynamic interaction of high speed train and railway structure including derailment during an earthquake. *Procedia Eng* 199:2729–2734
- Goto K, Sogabe M, Tanabe M et al (2018) Simple method for analyzing contact between wheelset members and track structures using MBD. *Q Rep RTRI* 59(1):57–64
- Wu X, Chi M, Gao H et al (2016) Post-derailment dynamic behavior of railway vehicles travelling on a railway bridge during an earthquake. *Proc Inst Mech Eng Part F J Rail Rapid Transit* 230(2):418–439
- Gottschalk S, Lin MC, Manocha D (1996). OBBTree: a hierarchical structure for rapid interference detection. In: Proceedings of the 23rd Annual Conference on Computer Graphics and Interactive Techniques, pp 171–180, New York

44. Eberly D. (2016) Dynamic collision detection using oriented bounding boxes. http://gingaminga.com/Data/Note/oriented_bounding_boxes/DynamicCollisionDetection.pdf. Accessed 2 June 2022.
45. Anderson RJ (1997) A train derailment simulation software package. Queen's University, Dynamics laboratory report
46. Jeong D, Lyons M, Orringer O et al (2007) Equations of motion for train derailment dynamics. In: ASME 2007 Rail Transportation Division Fall Technical Conference, pp 21–27, Chicago
47. Boronenko Y, Orlova A, Iofan A et al (2006) Effects that appear during the derailment of one wheelset in the freight wagon: simulation and testing. *Veh Syst Dyn* 44(sup1):663–668
48. Zhu X, Lu X-Z, Cheng Q-L et al (2020) Simulation of the running attitude of a train after derailment. *Int J Crashworthiness* 25(2):213–219
49. Ling L, Dhanasekar M, Wang K et al (2019) Collision derailments on bridges containing ballastless slab tracks. *Eng Fail Anal* 105:869–882
50. Kim S-W (1999) Contact dynamics and force control of flexible multi-body systems. Dissertation, McGill University.
51. Yao S, Zhu H, Liu M et al (2020) A study on the frontal oblique collision-induced derailment mechanism in subway vehicles. *Proc Inst Mech Eng Part F J Rail Rapid Transit* 234(6):584–595
52. Luo F, Liu C, Sun Z (2009) Intelligent vehicle simulation and debugging environment based on physics engine. In: 2009 International Asia Conference on Informatics in Control, Automation and Robotics, pp 329–333, Bangkok
53. Cho HJ, Koo JS (2012) A numerical study of the derailment caused by collision of a rail vehicle using a virtual testing model. *Veh Syst Dyn* 50(1):79–108
54. Bae H-U, Yun K-M, Lim N-H (2018) Containment capacity and estimation of crashworthiness of derailment containment walls against high-speed trains. *Proc Inst Mech Eng Part F J Rail Rapid Transit* 232(3):680–696
55. Sakdirat K, Wang Y, Ngamkhanong C (2018) Derailment-resistant performance of modular composite rail track slabs. *Eng Struct* 160:1–11
56. Zhou H, Wang W, Hecht M (2013) Three-dimensional derailment analysis of a crashed city tram. *Veh Syst Dyn* 51(8):1200–1215
57. Ling L, Guan Q, Dhanasekar M (2017) Dynamic simulation of train-truck collision at level crossings. *Veh Syst Dyn* 55(1):1–22
58. Zhou H, Zhang J, Hecht M (2014) Three-dimensional derailment analysis of crashed freight trains. *Veh Syst Dyn* 52(3):341–361
59. Brabie D (2005). On the influence of rail vehicle parameters on the derailment process and its consequences. Dissertation, KTH Royal Institute of Technology,
60. Brabie D (2007) Wheel-sleeper impact model in rail vehicles analysis. *J Syst Des Dyn* 1(3):468–480
61. Ling L, Dhanasekar M, Thambiratnam DP (2018) Dynamic response of the train–track–bridge system subjected to derailment impacts. *Veh Syst Dyn* 56(4):638–657
62. Tanabe M, Wakui H, Sogabe M et al (2010) A combined multi-body and finite element approach for dynamic interaction analysis of high-speed train and railway structure including post-derailment behavior during an earthquake. In: 9th World Congress on Computational Mechanics and 4th Asian Pacific Congress on Computational Mechanics, Sydney
63. Tanabe M, Sogabe M, Wakui H et al (2016) Exact time integration for dynamic interaction of high-speed train and railway structure including derailment during an earthquake. *J Comput Nonlinear Dyn* 11(3):031004
64. Ling L, Dhanasekar M, Thambiratnam DP (2017) Frontal collision of trains onto obliquely stuck road trucks at level crossings: derailment mechanisms and simulation. *Int J Impact Eng* 100:154–165
65. Tanabe M, Goto K, Watanabe T et al (2017) An efficient contact model for dynamic interaction analysis of high-speed train and railway structure including derailment during an earthquake. *Int J Transp Dev Integr* 1(3):540–551
66. Lankarani HM, Nikravesh PE (1994) Continuous contact force models for impact analysis in multibody systems. *Nonlinear Dyn* 5(2):193–207
67. Hajdin N, Mandic R, Miskovic Z (1996) Computer aided analysis of train impact on structures adjacent to the track. In: Proceedings of the Third International Conference on Computational Structures Technology, Budapest, pp 133–137
68. Paetsch C, Perlman AB, Jeong D (2006) Dynamic simulation of train derailments. In: ASME International Mechanical Engineering Congress and Exposition, pp 105–114, Chicago
69. Schupp G, Weidemann C, Lutz M (2004) Modelling the contact between wheel and rail within multibody system simulation. *Veh Syst Dyn* 41(5):349–364
70. Pogorelov D, Yazykov V, Lysikov N et al (2017) Train 3D: the technique for inclusion of three-dimensional models in longitudinal train dynamics and its application in derailment studies and train simulators. *Veh Syst Dyn* 55(4):583–600
71. Brabie D, Andersson E (2008) An overview of some high-speed train derailments: means of minimizing consequences based on empirical observations. *Proc Inst Mech Eng Part F J Rail Rapid Transit* 222(4):441–463
72. Brabie D, Andersson E (2008). High-Speed train derailments: minimizing consequences through innovative design. In: The 8th World Congress of Railway Research (WCRR 2008), Seoul
73. Zhai W, Wang K, Cai C (2009) Fundamentals of vehicle–track coupled dynamics. *Veh Syst Dyn* 47(11):1349–1376
74. Song IH, Kim J, Koo JS et al (2019) Simplified vehicle modeling technique for design of derailment containment provisions (DCP). *J Korean Soc Railw* 22(7):527–537
75. Zhai W, Han Z, Chen Z et al (2019) Train–track–bridge dynamic interaction: a state-of-the-art review. *Veh Syst Dyn* 57(7):984–1027
76. Asanuma K, Sogabe M, Watanabe T et al (2009) Development of ballasted ladder track equipped with a vehicle guide device. *Q Rep RTRI* 50(4):233–240
77. Bae H-U, Yun K-M, Moon J et al (2018) Impact force evaluation of the derailment containment wall for high-speed train through a collision simulation. *Adv Civ Eng* 2018:1–14
78. Shu X, Wilson N (2007) TCRP research results digest 82: use of guard/girder/restraining rails. Transportation Research Board, Washington DC
79. Tang Z, Yuan X, Xie X et al (2019) Implementing railway vehicle dynamics simulation in general-purpose multibody simulation software packages. *Adv Eng Softw* 131:153–165
80. Nie Y, Tang Z, Liu F et al (2018) A data-driven dynamics simulation framework for railway vehicles. *Veh Syst Dyn* 56(3):406–427
81. Tang Z, Zhu YR, Nie Y et al (2017) Data-driven train set crash dynamics simulation. *Veh Syst Dyn* 55(2):149–167